Eur Biophys J (1996) 24: 300–310

ARTICLE

Mathias Göschl · Serge Crouzy · Yves Chapron

Molecular dynamics study of an α-cyclodextrin-phosphatidylinositol inclusion complex

Received: 14 September 1995 / Accepted in revised form 11 March 1996

Abstract Cyclodextrins are cyclic oligosaccharides known for their ability to include substrate molecules in their hydrophobic cavity. Moreover, cyclodextrins show a hemolytic activity when mM concentrations are added to blood. This hemolysis is commonly interpreted as a massive dissociation of phospholipids from the cell membrane due to the formation of complexes with the cyclodextrins. In the literature, a complexation between α-cyclodextrin (α CD) and phosphatidylinositol (PI) specific to the inositol headgroup has been proposed. But the need for the detailed interaction mechanism between the two molecules motivated the present work based on molecular dynamics simulations. Investigation of long range electrostatic interactions shows that a mutual approach of the molecules is only possible when the primary hydroxyl side of α CD faces the inositol headgroup of PI. This orientation is also the most favourable from adiabatic- and free-energy profiles calculated along a reaction coordinate that leads to an inclusion of PI into α CD. For free energy simulations, partial hydration of the model has been used. A study of glycosidic bond dihedral angles in α CD shows an increase in dihedral fluctuations before complexation and a dihedral "freezing" once the complex is formed.

Key words α-Cyclodextrin · Inositol-lipids · Inclusion complex · Molecular dynamics · Free energy calculations

Introduction

Cyclodextrins are cyclic oligosaccharides formed by a closed ring of glucose residues. They form a hydrophobic cavity whose dimensions depend on the number of glucose residues. Their toroid shape stems from a characteristic hydrogen bonding pattern and the conformation of the torsion angles in the glycosidic bonds. The most frequently studied α-, β-, and γ-cyclodextrins (with respectively 6, 7 or 8 glucose residues) are known to act as *host*-molecules for a great number of inclusion complexes with different organic *guests* (e. g. for α-cyclodextrin (α CD): methanol (Hingerty and Saenger 1975), azo-dyes (Cramer et al. 1967)). This property has been frequently used in the pharmaceutical industry to increase the efficiency of drugs by altering their solubility and surface activity (Saenger 1980). An important biomedical aspect of cyclodextrins is their hemolytic character: it has been observed, that cyclodextrins increase the erythrocytic membrane permeability (Szejtli et al. 1986) and that β-, α-, and γ-cyclodextrins, ranked in decreasing order of efficiency can induce hemolysis at mM concentrations (Irie et al. 1982). Cyclodextrins are supposed to be able to pull phospholipids out of the cell membrane to form lipid-CD complexes. This complex-mediated extraction of lipids from the membrane may then result in the rupture of the erythrocytic membrane (Ohtani et al. 1989; Irie et al. 1982; Szejtli et al. 1986). Experiments on the cyclodextrin induced release of lipids from the membrane show that α CD acts most efficiently on phospholipids whereas β CD interacts with cholesterol lipids (Ohtani et al. 1989). Moreover, a NMR study demonstrates that α CD interacts very strongly with phosphatidylinositol (PI), and only weakly with phosphatidylcholine (Fauvelle et al. 1994). The direct implication of the inositol headgroup in the complexation mechanism is proposed for phospholipid recognition at the membrane level and is confirmed in our study of α CD-*myo*-inositol phosphate interaction (Crouzy et al. 1996). The NMR results together with equivalent observations from other authors (Szejtli et al. 1986) suggest that the nature of the lipid headgroup is one decisive factor in the ability of cyclodextrins to form complexes with phospholipids. However, the structural details of such as complex remain unclear: in the papers cited above, various arguments are given in favour of head inclusion, loose association or even inclusion of the lipid alkyl chains.

M. Göschl (✉) · S. Crouzy · Y. Chapron
Laboratoire de Biophysique Moléculaire et Cellulaire,
Département de Biologie Moléculaire et Structurale,
Centre d'Etudes Nucléaires de Grenoble, 17, rue des Martyrs,
F-38054 Grenoble Cedex, France
(email: goeschl@arve.ceng.cea.fr)

In this work, an attempt is made to elucidate the possible structure of a complex between αCD and PI, the latter being chosen for their strong interaction and the availability of a small set of NMR data. Although the three-dimensional structure of the entire complex cannot yet be found, the knowledge of the x-ray structures of αCD, inositol and the phospholipid backbone allows us to use molecular dynamics (MD) and modeling techniques for our study. A partially hydrated model is used as a compromise between correct representation of solvation effects and computational cost. Of special interest is the estimation of the electrostatic (long range) interaction between the molecules during a distant *first approach*. Further investigation by energy minimization and free energy techniques within the closer range of Van der Waals (VDW) contacts helps one decide whether or not stable conformations exist as inclusion complexes. These complexes are best characterized by their hydrogen bonding pattern and the value of the glycosidic bond dihedral angles in αCD. Our approach to a specific lipid-CD interaction should be helpful to study the mechanism of the complexation between cyclodextrins and lipids in general.

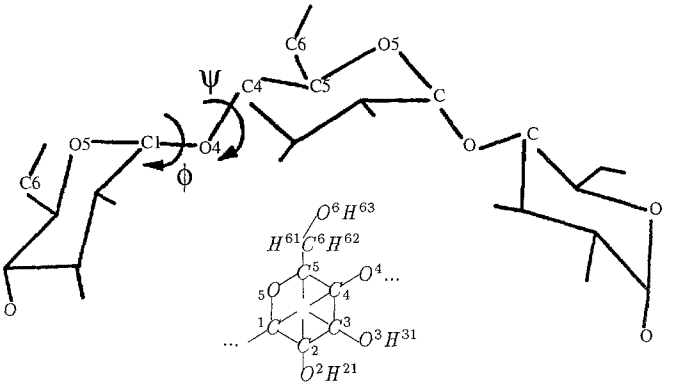

Fig. 1 Topology of cyclodextrins. Glucose residues are linked between their $C_{(1)}$ and $C_{(4)}$ atoms to form a closed ring. Dihedral angles Φ/Ψ are defined in the glycosidic bond. In the center, a complete nomenclature of one glucose residue is given (hydrogens $H_{(n)}$ linked to carbons $C_{(n)}$ of the ring are shown as strokes without atom name)

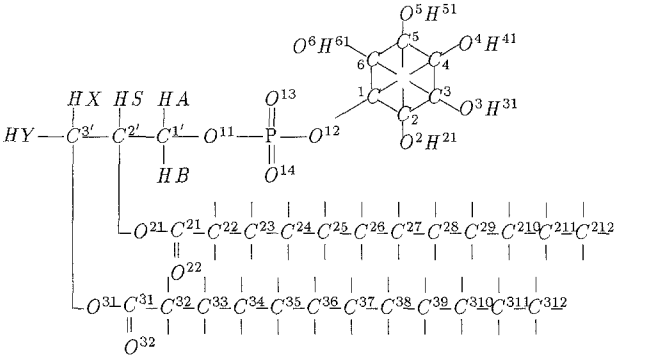

Fig. 2 Topology of 12,12-dilauroyl-phosphatidylinositol. Hydrogens in the lipid chains are treated in an extended carbon atom representation. Hydrogens $H_{(n)}$ linked to carbons $C_{(n)}$ in the inositol ring are shown as strokes without atom name. For the sake of drawing simplicity, the positions of the atoms (in particular, the lipid chains) does not reflect the real 3 D structure

Methods

Molecular model

The initial αCD coordinates of all non-hydrogen atoms are taken from crystallographic data (Manor and Saenger 1974). Each glucose residue is linked to its neighbours by two $\alpha(1-4)$ glycosidic bonds. The dihedral angles $\Phi \mapsto O_5-C_1-O'_4-C'_4$ and $\Psi \mapsto C_1-O'_4-C'_4-C'_5$ are defined to monitor the arrangement of the glucose residues (Fig. 1). Two sides of αCD can be distinguished: the "mOH"-side bearing the primary hydroxyl groups $C_{(6)}H_{(61,\,62)}O_{(6)}H_{(63)}$, and the "OH"-side (secondary hydroxyl groups $O_{(2)}H_{(21)}$ and $O_{(3)}H_{(31)}$). In the cyclodextrin ring, a total of 3 hydroxyl groups per glucose residue provide donors for hydrogen-bonding based stabilisation of the macrocycle and the possibility of a flexible bonding scheme with other organic compounds in contact with αCD (Myles et al. 1994).

The structure of PI consists of a *myo*-inositol ring which is linked with its $C_{(1)}$-carbon to the phosphate group of the phospholipid backbone (Fig. 2). Coordinates were taken from x-ray data of *myo*-inositol-dehydrate (Rabinowitz and Kraut 1964) for the ring and from the phospholipid backbone of 1,2-dilauroyl-phosphatidyl-ethanolamine (DLPE) (Elder et al. 1977).

Basic computational procedures

All MD simulations were carried out using the CHARMM force-field (Brooks et al. 1983). Missing hydrogen coordinates were built using the CHARMM HBUILD command with default settings. To reduce the total number of atoms, extended carbone representation was used for CH_2 and terminal CH_3 groups of the hydrocarbon tails in PI. The SHAKE method (van Gunsteren and Berendsen 1977) was applied to constrain bond-lengths between heavy atoms and hydrogens. Dynamic runs were performed using Langevin dynamics with a $T=300$ K heatbath (friction coefficient on non-hydrogen atoms: 10 ps^{-1}) and a 1 fs integration timestep. Nonbonded interaction cutoff was set to 15 Å (no cutoff was used during *first approach* simulations). Hydrogen bonds were treated explicitly with a CHARMM 4–6 potential (well depth: 4.25 kcal/mol, distance: 2.75 Å for oxygens) and 4 Å cutoff. Partial charges were calculated using an iterative procedure combining semi-empirical quantum mechanics Mulliken population analysis at the MNDO level of theory using the MOPAC program (Dewar and Thiel 1977) and Adopted Basis Newton Raphson (ABNR) geometry optimizations with CHARMM (Brooks et al. 1983). At each iteration step, initial coordinates are provided and charges calculated with MOPAC without geometry optimization, then an

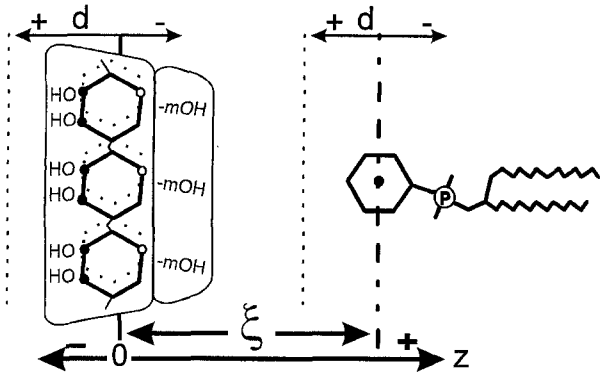

Fig. 3 Schematic representation of αCD and PI in the (αCD)-mOH$\leftrightarrow$inositol-(PI) orientation. The two sides of αCD namely "OH"and "mOH", are *highlighted.* ξ is the reaction coordinate, defined as the distance between the center-of-mass plane of αCD and the center of the inositol ring. *d* is the distance between a test plane and each molecule used for the computation of electrostatic potential charts

energy minimized structure is computed with CHARMM using these charges and serves as the initial structure for the next step. The procedure is stopped when the rms differences between coordinates and charges of successive steps are smaller than 10^{-3} Å and 10^{-4} charge units respectively.

Partial charges for the glycerol group of PI were taken from the CHARMM22 file: top_all22_lipid and set to zero for the $C_{(2n,3n)}$ ($n > 2$) PI chain carbons to take into account the global neutrality of CH_2 and CH_3 groups. Charges on all other atoms of PI and αCD were initially set to zero and refined until convergence using the procedure described in the previous paragraph, within a few steps. In the case of αCD, a set of charges evenly distributed among all glucose residues was obtained. The total charge of αCD is 0 whereas the total charge of PI, located on the phosphate group, is –1.

Force constants and non-bonded interaction parameters for PI were taken from the CHARMM22 file: par_all22_lipid. Equilibrium values for dihedrals in the phosphate-inositol link were set to the values suggested by Hansbro et al. (1992). In the case of αCD, force-field parameters were taken from the QUANTA library for glucose molecules and were similar to those proposed by other workers (Koehler et al. 1987).

Final charges of both molecules are given in Table 1. Charges calculated using our iterative procedure differ only slightly from the values that can be found in the QUANTA parameter files (0.04 charge units r.m.s. difference for all polar oxygens and hydrogens involved in hydrogen bonding in αCD). These minor changes, however, ensure a high compatibility between the semi-empirical force-field used to derive these charges and the molecular mechanical force-field used to energy minimize the structure. Neither of these force fields has been changed for our study. Only unknown equilibrium values and force constants for a few dihedral angles have been taken from the literature or from QUANTA.

Table 1 Partial charges of αCD and PI

αCD[a]		PI	
Atom	q	Atom	q
$C_{(1)}$	0.28	$C_{(1)}$	0.09
$C_{(2)}$	0.05	$C_{(2,\ldots,6)}$	0.07
$C_{(3)}$	0.07	$O_{(2,\ldots,6)}$	–0.39
$C_{(4)}$	0.12	$H_{(1,3,5)}$	0.06
$C_{(5)}$	0.05	$H_{(2,4,6)}$	0.08
$C_{(6)}$	0.11	$H_{(21,61)}$	0.27
$O_{(2)}$	–0.38	$H_{(31,41,51)}$	0.23
$O_{(3)}$	–0.40	P	1.34
$O_{(4)}$	–0.42	$O_{(11,12)}$	–0.58
$O_{(5)}$	–0.38	$O_{(13,14)}$	–0.66
$O_{(6)}$	–0.39	$C_{(1')}$	–0.08
$H_{(1)}$	0.11	$C_{(2')}$	0.04
$H_{(2)}$	0.10	$C_{(3')}$	–0.05
$H_{(3)}$	0.07	HA, HB	0.04
$H_{(4)}$	0.08	HS	0.09
$H_{(5)}$	0.08	$O_{(21,31)}$	–0.34
$H_{(21)}$	0.25	$C_{(21,31)}$	0.63
$H_{(31)}$	0.25	$O_{(22,32)}$	–0.52
$H_{(61)}$	0.08	$C_{(22,32)}$	0.10
$H_{(62)}$	0.04	HX, HY	0.09
$H_{(63)}$	0.23	$C_{(2n,3n)}$ $n > 2$	0.00

[a] Charges are equivalent for all six residues

Both molecules were oriented with their principal axis aligned with the *z*-axis and the center of mass (c.o.m.) of αCD was set to the origin of the coordinate system (see Fig. 3). For partial hydration of the model, a sphere ($r = 11.5$ Å) of TIP3P water molecules (Jorgensen et al. 1983), centered at the origin and confined by a stochastic boundary potential (Brooks and Karplus 1983) was added to the simulation system. Water molecules with oxygens closer than 2.8 Å to a heavy atom of PI or αCD were removed.

Practical implementation

The study of intermolecular attraction or complexation has been divided into two major parts: i) long range electrostatic effects and ii) short range multiple (Van der Waals, electrostatic, hydrogen-bond) interactions. Additionally, the conformational space sampled by the αCD glycosidic bond dihedral angles Φ/Ψ provides a key to the analysis of the deformation of αCD upon complexation with PI.

Long range interaction

Electrostatic potentials. To investigate how α CD can "feel" the presence of a PI molecule, even several Å away, and in which way this may lead to a directed *first approach,*

the electrostatic potential in the vicinity of both molecules was computed from the interaction energy of a $q=1$ test-charge with the molecular structure. The charge was localized on planes defined by a normal vector $\mathbf{n}=(0,0,1)$ and a point $\mathbf{P}=(0,0,d)$ where d is given in Å. $d=0$ refers to the center of mass of αCD or the center of geometry of the six carbons constituting the inositol ring of PI as shown in Fig. 3.

Distant approach dynamics. Two pathways corresponding to two opposite orientations of αCD with respect to PI were defined for the complexation process: pathway (I) for a contact between the mOH side of αCD and the inositol ring, pathway (II) for a contact between the OH side of αCD and the PI ring. To study how electrostatic forces can steer a distant *first approach*, simulations consisting of 150 ps dynamics runs, one for each initial orientation (I/II), were computed in the absence of explicit waters but using a dielectric constant $\varepsilon=80$ and no cutoff. The initial distance between the molecules was set to 40 Å. The phosphorus atom of PI and the two terminal carbons of the hydro carbon tails were kept fixed during the simulation and the diffusion of free αCD towards PI was monitored.

Short range interaction

An inclusion reaction can be described by a simple (linear) reaction coordinate: the distance between *guest* and *host*. In the present study, the c.o.m. of αCD was constrained at the origin of the coordinate system and one $O_{(4)}$-oxygen atom was restrained by a weak harmonic potential to prevent free rotation of αCD. A reaction coordinate ξ was defined as the distance between the c.o.m. plane of αCD and the center of geometry of the inositol ring (Fig. 3). Independent of the orientation of the two molecules, PI was translated towards αCD from $+z$ to $-z$.

Adiabatic energy profiles. To study intermolecular interactions between αCD and PI (no hydration, $\varepsilon=1$), ABNR energy minimizations were carried out with the reaction coordinate constrained by a strong "planar" harmonic potential (10^4 kcal mol^{-1} Å^{-2}). To improve the exploration of the energy surface and taking account of the 6-fold symmetry of αCD, PI was rotated around its principal axis from 0 to 60 degrees in steps of 15 degrees. At each turn-step, harmonic restraints were set up for the inositol ring and phosphate atoms to temporarily hold PI in place, then slowly removed in an iterative procedure where the structure was heated to 300 K then cooled down to 0 K and minimized. Following this annealing procedure, the structure of lowest total energy over all turns was retained.

Free energy profiles and reaction rates. Evaluation of barrier crossing rates implies the calculation of free energy profiles along the reaction coordinate. Profiles were calculated both in the gas phase and in the presence of water molecules, but only the latter will be presented. The *umbrella-sampling* technique (Patey and Valleau 1975; Crouzy et al. 1994; see Theory section) was used with planar umbrella-potentials (force constant: 110 kcal mol^{-1} Å^{-2}) centered at reaction coordinate values ξ ranging from −8 to 8 Å in steps of $\Delta\xi=0.1$ Å. For each ξ, the structure was minimized with 500 steps ABNR, then heated from 0 to 300 K in 1 ps prior to a 25 ps (25 000 steps) Langevin dynamics production run at 300 K. The probabilities $P_{(\xi(t)=\xi)}$ were evaluated after binning the values $\xi(t)$, stored every fs, into normalized histograms (overlapping of the histograms corresponding to adjacent umbrella windows was carefully checked to optimize the strength of the biasing potential). The final free energy profile is a weighted average of all the $^{\circ}W_i(\xi)$ for all windows i (Crouzy et al. 1994). For the evaluation of reaction rates from free energy barrier heights, transition state theory was used. The necessary frequency factors and diffusion constants were calculated using the Kramers-Smoluchowsky relation and a Generalized Langevin Equation approach, respectively.

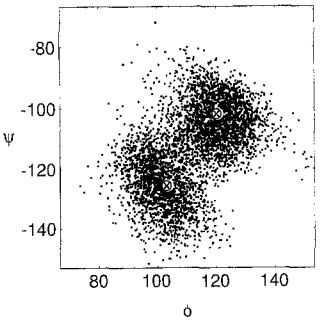

Fig. 4 Distribution of the Φ/Ψ dihedral angles in αCD (see Fig. 1) during 15 ps. dynamics trajectories at 300 K calculated in the gas phase. *Crossmarks* indicate the two Φ/Ψ populations present in the minimized αCD vacuum structure

Structural study

Proton distances and hydrogen bonding. Some interproton distances for the complex PI-αCD are available from ^{1}H-NMR spectroscopy (Fauvelle et al. 1994). To assess the validity of our model structures corresponding to lowest energy wells on the free energy profiles, these average distances have been calculated from 100 ps dynamics trajectories at 300 K. From the same simulations, donor-acceptor distances with an average CHARMM H-bond energy less than −1.5 kcal/mol have also been computed.

Conformation of αCD. To obtain information on the conformational behaviour of glycosidic bond dihedral angles in the αCD molecule alone and during the approach of PI, Φ/Ψ were extracted every 20 fs from 15 ps dynamics trajectories calculated with and without hydration and for both orientations I/II at various values of ξ. Except for the force constant of the constraining potential of ξ (now set to 10^4 kcal mol^{-1} Å^{-2}), all simulation parameters were identical to those described for the free energy simulations. Φ/Ψ-pairs were binned into 2 D-histograms on a 4×4 degree grid. Significant peaks in the histograms were calculated as the statistical average of (Φ, Ψ) values weighted by the height of their corresponding bin on a 7×7 bin wide "peak-area". This area was defined as having the central bin dominating all its surrounding 48 neighbours by at least

15%. The global Φ/Ψ mean value, standard deviation and significant peaks were extracted for each histogram.

Theory

Free energy calculations

In general, the free energy along a reaction coordinate ξ (also called: potential of mean force) is approximated by

$$\mathcal{W}_{(\xi=\xi_1)} = -k_B T \ln P_{(\xi=\xi_1)} = -k_B T \ln \frac{\int \ldots \int e^{-\beta E(\mathbf{R})} \delta(\xi_{\mathbf{R}} - \xi_1)\, d\mathbf{R}}{\int \ldots \int e^{-\beta E(\mathbf{R})} d\mathbf{R}} \quad (1)$$

where $P_{(\xi=\xi_1)}$ is the probability of finding the reaction coordinate around a given value ξ_1. To enhance the sampling in the neighbourhood of a reference value ξ_0, a harmonic biasing potential centered at ξ_0: $u_i(\xi) = \frac{k}{2}(\xi - \xi_0)^2$ is introduced (Umbrella sampling). The unbiased potential of mean force is then

$$\mathcal{W}_i(\xi_1) = -k_B T \ln P^b_{i(\xi=\xi_1)} - u_i(\xi_1) + \mathcal{C}_i$$

$$\mathcal{C}_i = k_B T \ln \langle e^{-\beta u_i(\xi_1)} \rangle \quad (2)$$

where $P^b_{i(\xi=\xi_i)}$ is the biased probability function of ξ under the biasing potential $u_i(\xi)$. The constant terms $\mathcal{C}_i$ can be calculated by combining the results from different windows (Crouzy et al. 1994). Once a free energy profile is known, the transition rate between two stable states is given by

$$k = F_p\, e^{-\Delta \mathcal{W}/k_B T} \quad (3)$$

where $\Delta\mathcal{W}$ is the activation free energy barrier and F_p is called the pre-exponential frequency factor. The latter can be calculated from $\mathcal{W}$ using the Kramers-Smoluchowsky relation (Kramers 1940) that gives an appropriate approximation in the high friction regime. This calculation necessitates the evaluation of the average diffusion constant within the barrier. Here, we use a technique based on the analysis of the Generalized Langevin Equation (Berne et al. 1988; Woolf and Roux 1994). For a detailed description of the procedure, the reader is refered to Crouzy et al. (1994).

Results

Long range interaction

Electrostatic potentials

The computation of electrostatic potential maps for αCD at $d = 0$ Å yields 6 equivalent peaks in a 6-fold symmetry, reflecting the homogeneity of the αCD structure. The residues globally bear a negative charge, the outer region of the ring forms a positive "corona". The apolar cavity (potential energy $|E_{ele}| < 3.5$ kcal/mol.) can clearly by distinguished (Fig. 5 a). The peaks seen at $d = 0$ Å vanish for $|d| > 5$ Å. Potential maps for αCD calculated further away ($d = \pm 8$ Å, see Fig. 5 c, d) illustrate the dipolar character of the entire molecule: the "mOH" side bears a global positive charge, whereas the "OH" side appears to be charged negatively. Coulomb-maps for PI show the polar character of the molecule down to distances of $d = 2.5$ Å where a structured image of the inositol ring is about to appear. When viewed from above a fictive membrane surface ($d > 0$), PI appears to be charged negatively (see Fig. 5 b). The electric dipole moments, calculated by QUANTA, for αCD and PI are 1.02 Debye and 23.41 Debye, respectively. The dipole vector of α CD is parallel to the main axis of the molecule and points in the direction OH to mOH. The dipole moment of PI points from the inositol-head to the phospholipid-tail and also nearly coincides with the main axis of the molecule.

Distant approach dynamics

From the "first approach" trajectories described under Methods, the following behaviour has been observed by molecular graphics: For orientation (I), initial distance $\xi = 40$ Å, αCD approaches PI and gets in contact after $t \sim 90$ ps. During the approach, the dipoles of the two molecules remain parallel. α CD stays face to face to PI for about 35 ps and then starts tilting aside towards a configuration with antiparallel dipole orientations where the two molecules sit on top of each other. At this stage, hydrogen bonds are found for: $O_{(2)}H_{(21)}\cdots O_{(13)}$ and $O_{(3)}H_{(31)}\cdots O_{(22,\,32)}$ (α CD$\cdots$PI). Further 50 ps of dynamics calculated with lipid tails now entirely released showed an occasional inclusion of one hydrocarbon tail of PI into the cavity of α CD. In the case of initial orientation (II), α CD first repulsed by PI, turns around by ~180° where it now feels attractive forces from PI and the continues its final approach as described for orientation (I).

Short range interaction

Adiabatic energy profiles

From the minimum energy profiles computed for orientations I and II in the absence of water molecules and shown in Fig. 6, a barrier of ~40 kcal/mol for the PI headgroup entering the cavity of α CD is observed. Rotation steps smaller than 15 degrees did not significantly alter this result. Two energy wells for ξ around 2 to 4 Å and for ξ around –3 to –6 Å (the so called partially- and fully-complexed states) can be distinguished. Values of $\xi \lesssim -10$ Å, correspond to the penetration of the two hydrocarbon tails of PI into αCD and result in very high VDW energies owing to steric clashes. Decomposition of the PI-αCD interaction energy (no intramolecular terms) into its electro-

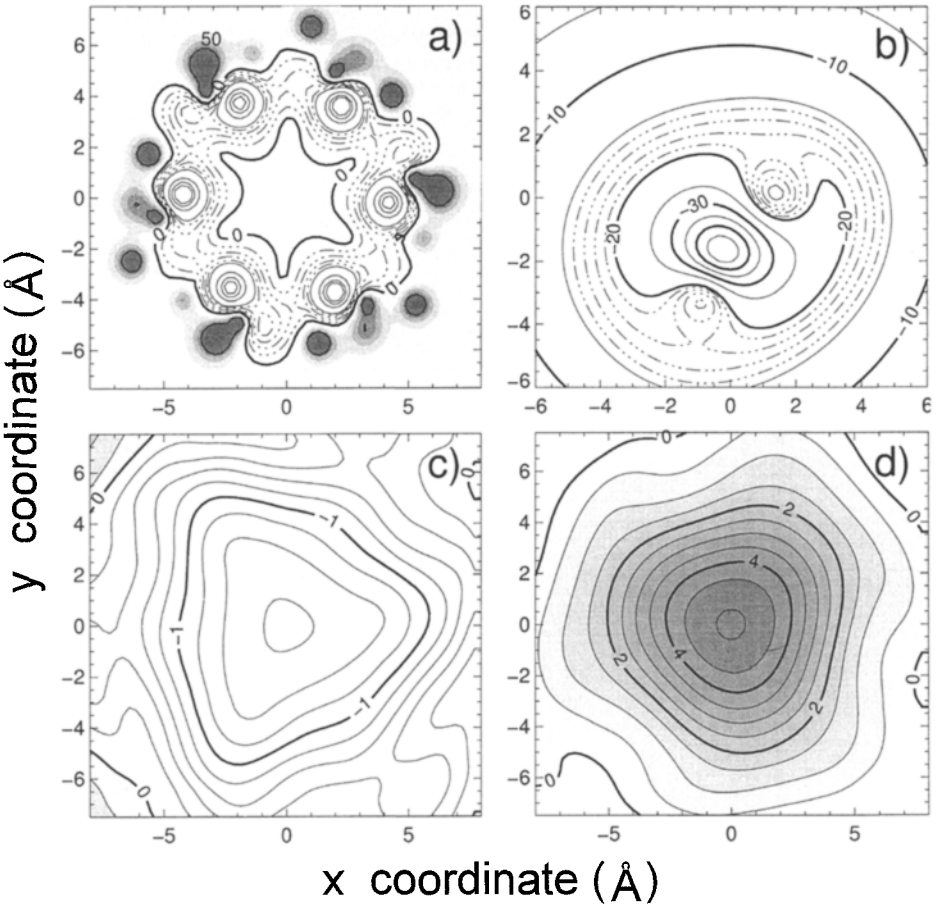

Fig. 5a–d Electrostatic potential charts calculated on planes at fixed distances d from αCD (or PI) (see Fig. 3). **a** αCD seen from $d=0$. The apolar center of the cavity and the six charged glucose units can clearly be identified. **b** Headgroup of PI seen from $d=+3.0$ Å. A global negative charge appears. Asymmetries seen within the dashed levels are due to the $O_{(3)}H$ and $O_{(5)}H$ groups. **c** αCD seen from $d=+8$ Å (OH-side), is globally negatively charged. **d** αCD seen from $d=-8$ Å (mOH-side). The global charge appears to be positive. The scaling of the planes is given in Å. Areas of positive energy are rendered in *greyscales,* areas of negative energies are coloured *white.* In **a**, *dashed contours* and *greylevels* are separated by 10 kcal/mol, solid lines are drawn at 50 kcal/mol intervals. In **b** to **d**, levels are indicated or can be extrapolated with the help of different line widths and styles

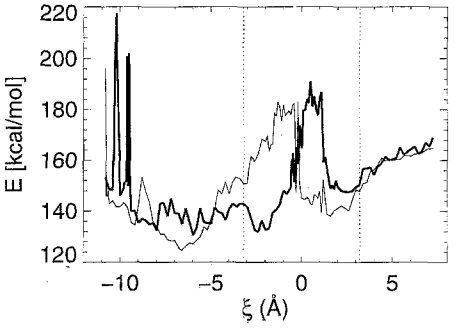

Fig. 6 Adiabatic energy profiles for the inclusion of PI inositol headgroup into the αCD cavity calculated along the ξ reaction coordinate (see Fig. 3). The *thick line* corresponds to orientation (I), (αCD)-mOH$\leftrightarrow$inositol-(PI), and the *thin line* to orientation (II). The *grey shaded area* schematically represents the dimension of the αCD molecule

static and VDW terms, reveals that VDW interaction contributes most to the energy entrance barrier. For both orientations, VDW energy decreases within the cavity and the minimal total interaction energy of the fully complexed state is more than 10 kcal/mol lower than that of the partially complexed state.

Free energy profiles and reaction rates

Free energy profiles calculated along ξ for orientations (I) and (II), are shown in Fig. 7a, b) respectively. For initial orientation (II), a large energy barrier of $\Delta E=43.3$ kcal/mol is found for PI entering the cavity of α CD. On the other hand, for orientation (I), the barrier leading to the fully complexed state is considerably lower and the well corresponding to the partially complexed state is very shallow with a barrier height of 15.2 kcal/mol. While for orientation (I), the height of the dissociation barrier, 35.6 kcal/mol, clearly favours the fully complexed state, the situation is different for orientation (II) where the partially complexed state appears to be more stable. For both orientations, the barrier-tops are located at ξ close to zero and for values of $\xi<-7.5$ Å, free energy increases strongly. For $\xi>5$ Å, free energy also increases mainly owing to less and less attractive VDW forces. This is especially true in the case of orientation (II) where the partially complexed state, consequently, appears very stable. From a set of preliminary simulations, it was observed that the shape of the profiles is only slightly influenced by the choice of the initial lipid turn-angle at the beginning of an "umbrella" run. Positions and heights of free energy barriers are summarized in Table 2.

Table 2 Energy barriers, diffusion constants and transition rates for orientations (I) and (II). $\xi_{i/o}$ denote positions of the energy wells for the fully (in) and partially (out) complexed states; ξ_b is the main barrier position and $\tilde{D}$ the average diffusion constant in the barrier. $\Delta E_{o\to i}$ is the activation free energy from the partially to the fully complexed state (resp. $\Delta E_{i\to o}$ from fully to partially complexed state), $F_p^{o\leftrightarrow i}$ and $k_{o\leftrightarrow i}$ the corresponding frequency factors and transition rates

ξ_o	ξ_b	ξ_i	$\Delta E_{o\to i}$	$\Delta E_{i\to o}$	$\tilde{D}$	$F_p^{o\to i}$	$F_p^{i\to o}$	$k_{o\to i}$	$k_{i\to o}$
[Å]			[kcal/mol]		[Å^2/ps]	[$10^{12}\times$s^{-1}]		[s^{-1}]	
(I) (αCD)-mOH $\leftrightarrow$inositol-(PI):									
5.2	0.4	−2.4	15.2	35.6	0.071	0.52	1.20	4	1×10^{-14}
(II) (αCD)-OH $\leftrightarrow$inositol-(PI):									
2.9	0.3	−6.2	43.3	32.3	0.075	1.50	0.65	4×10^{-20}	2×10^{-12}

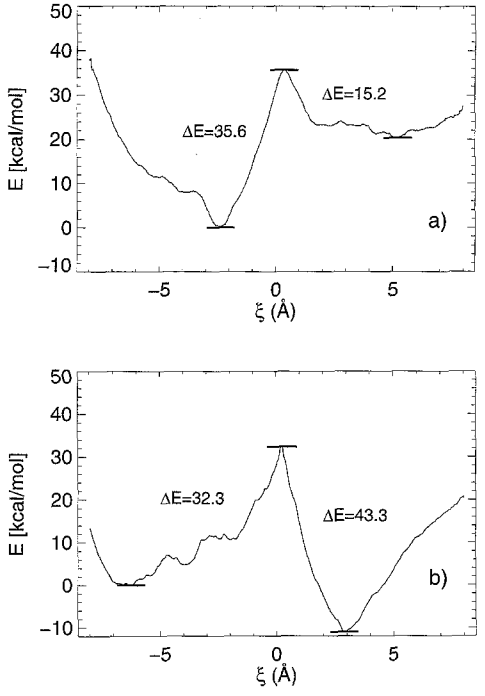

Fig. 7 a, b Free energy profiles for the inclusion of PI inositol headgroup into the αCD cavity calculated along the ξ reaction coordinate for orientation (I) (αCD)-mOH $\leftrightarrow$ inositol-(PI) (**a**) and orientation (II) (αCD)-OH $\leftrightarrow$ inositol-(PI) (**b**). The absolute minima of the free energy profiles have been set to zero

Diffusion constants have been calculated from 60 ps trajectories calculated at 300 K for three different values of ξ ($\xi=\xi_{top}$, $\xi_{top}\pm0.3$ Å) within each main energy barrier and averaged. The values of D in all energy barriers remain close to 0.07 Å^2/ps. The pre-exponential factor F_p is evaluated for the crossing of the main barriers separating the partially and fully complexed state. The results are listed in Table 2 and show that F_p is on the other of 10^{12} s^{-1}, similar to the theoretical value of k_BT/h known for a perfect gas phase. Transition rates k were calculated using Eq. (3) and are also listed in Table 2.

From these results it is clear, that full complexation is likely to happen only in orientation (I) for which the mOH-side of αCD and the headgroup of PI are opposed. Partial complexation from the OH side, orientation (II), is also possible, but, from electrostatic maps, it has been demonstrated that this orientation is very unlikely for long distance approach of the two molecules. Accordingly, the results reported below will mainly be focused on orientation (I) and for simulations done in the presence of waters.

Structural study

Proton distances and hydrogen bonding

Closest distances (≤2.5 Å) between H atoms from αCD and PI have been analysed and, for orientation (I), results are compiled in Table 4. Closest distances involving $H_{(3)}$ in αCD or HA, HB, HY in the glycerol part of PI are seen only in the fully complexed state.

The average hydrogen bonding pattern of the hydrated PI-αCD system in orientation (I) has been analysed and results are summarized in Table 3. At $\xi=3.0$ Å, when the inositol ring has not yet entered the cavity and stays close to the mOH-side of α CD, hydrogen bonds are found mainly between $O_{(2)}$ of one glucose residue and $O_{(3)}$ of the following glucose evenly around the αCD torus, and between $O_{(3,4)}$ of PI and $O_{(4)}$ of αCD. When $\xi=-2.5$ Å, the bonding pattern between $O_{(2)}$ and $O_{(3)}$ atoms in αCD is altered, owing to the elliptical shape of the molecule after complexation. Hydrogen bonds between residues in the two regions of low curvature of the torus are more stable than those found in the high curvature part. The lower bond energy is essentially due to an increase in the bond distance and unfavourable bonding angles. PI is mainly bound to αCD by hydrogen bonds between $O_{(2)}H\cdots O_{(5)}$, $O_{(2)}\cdots HO_{(2)}$ and $O_{(6)}H\cdots O_{(4)}$ (PI$\cdots\alpha$CD). Water molecules are hydrogen-bonded to the "front"-part of the inositol ring, namely to $O_{(3,4,5)}$.

Conformation of αCD

The overall minimized geometry of the αCD vacuum structure is perfectly circular with a diameter of 8.43 Å, measured between opposite $O_{(4)}$ atoms. In this state and during 100% of the simulation time (100 ps) at 300 K, the structure shows a characteristic hydrogen bonding pattern (Koehler et al. 1988) with six strong hydrogen bonds (bond

Table 3 Hydrogen bonds for the hydrated model in orientation (I): (αCD)-mOH↔inositol-(PI). Only long living and stable bonds between PI, αCD and H_2O (W) are given. ξ denotes the position of the reaction coordinate. M, R, A are the molecule-, residue- and atom-name of the H-bond donor/acceptor atoms, *d* the corresponding bond distance and E the bond energy averaged over 100 ps dynamics trajectories

	ξ [Å]	Donor			Acceptor			*d* [Å]	*E* [kcal/mol]	Remarks
		M	R	A	M	R	A			
1	−2.5	CD	n	$O_{(2)}$	CD	n+1	$O_{(3)}$	3.0	−3.2	n=1, 3, 4, 6 [a, b]
2	−2.5	CD	n	$O_{(2)}$	CD	n+1	$O_{(3)}$	3.3	−1.7	n=2.5 [c]
3	−2.5	PI	–	$O_{(2)}$	CD	4	$O_{(5)}$	2.9	−3.2	time: >15 ps
4	−2.5	PI	–	$O_{(6)}$	CD	2	$O_{(4)}$	3.2	−1.9	time: ~10 ps [c]
5	−2.5	CD	4	$O_{(2)}$	PI	–	$O_{(2)}$	3.1	−2.6	time: ~5 ps [c]
6	−2.5	PI	–	$O_{(m)}$	W	–	O	3.8	−1.6	m=3, 4, 5
1	3.0	CD	n	$O_{(2)}$	CD	n+1	$O_{(3)}$	3.0	−3.3	n=1 ... 6 [a]
2	3.0	PI	–	$O_{(3)}$	CD	5	$O_{(4)}$	3.2	−2.3	time: ~10 ps
3	3.0	PI	–	$O_{(4)}$	CD	3	$O_{(4)}$	3.1	−2.9	time: ~1 ps
4	3.0	PI	–	$O_{(m)}$	W	–	O	3.3	−2.3	m=2, 4, 5, 6

[a] reversed bond directions ("flip-flop") are also observed
[b] OH ··· HO double hydrogen bonds are frequent
[c] bad bond angle

Table 4 Close intermolecular H-H distance between PI and αCD in orientation (I): (CD)-mOH↔inositol-(PI)-and in the presence of solvent

H (PI)	H (αCD)	Distance (Å)
• ξ=3.0 Å		
$H_{(1, 2, 3)}$	$H_{(61, 62)}$	2.30
$H_{(3)}$	$H_{(5)}$	2.30
$H_{(4)}$	$H_{(5)}$	2.05
• ξ=−2.5 Å		
$H_{(2)}$	$H_{(3)}$	2.20
$H_{(3,5)}$	$H_{(3)}$	2.25
$H_{(21)}$	$H_{(3)}$	2.35
$H_{(6)}$	$H_{(3)}$	2.30
$H_{(61)}$	$H_{(3)}$	2.40
HA	$H_{(5, 62)}$	2.35
HB	$H_{(5, 61, 62)}$	2.25
HY	$H_{(62)}$	2.40

distance: ~3.0 Å, E ≃ 3.1 kcal/mol) present between $O_{(2)}H_{(21)}\cdots O_{(3)}$ in adjacent glucose residues. Upon hydration of the model, one to two water molecules can simultaneously be found inside the cavity (within the *z*-position of $O_{(6)}$ and $O_{(2, 3)}$), frequently H-bonded to an $O_{(6)}H_{(63)}$ group. This finding is consistent with the observations made by other authors (Saenger et al. 1976).

The glycosidic bond dihedral angles Φ and Ψ of minimized αCD in vacuum form two distinct populations in Φ/Ψ-space: $\overline{(\Phi/\Psi)}_1 = 120.3°/-101.9°$ and $\overline{(\Phi/\Psi)}_2 = 103.3°/-125.5°$. The two populations correspond to alternate values of Φ and Ψ from one sugar residue to the next in the ring. During dynamics at 300 K, these two populations can still be distinguished (Fig. 4). The Φ/Ψ-values and r.m.s. fluctuations averaged over all residues are: $\Phi = 111.6°$ (±12.5°) and $\Psi = -114.1°$ (±13.9°), values which are in good agreement with those found for related disaccharides ($\Phi/\Psi = 116.1°/-118.0°$) (Takusagawa and Jacobson 1978) or MD studies of βCD (Myles et al. 1994). Upon hydration, Φ/Ψ are slightly altered averaging now to: $\Phi = 108.6°$ (±8.8°) and $\Psi = -113.1°$ (±13.0°).

Computation of Φ/Ψ-distributions at 300 K, in the presence of PI and for different values of ξ, shows a strong effect of the position of PI on the dihedral fluctuations in the intercyclic glycosidic bonds of αCD. The behaviour of Φ/Ψ for the hydrated system in orientation (I) is summarized in Fig. 8. Three main observations can be highlighted: i) when the two molecules are far apart, Φ/Ψ logically fall into the two populations found for αCD alone; ii) when PI "tries" to overcome the main energy barrier leading to the fully complexed state, Φ/Ψ-fluctuations are strongly increased; iii) in the fully complexed state, Φ/Ψ are "freezed" into one single population located between the two reference equilibrium values. When comparing these results to those found for orientation (II) (not shown), the main difference is the absence of large Φ/Ψ fluctuations in the partially complexed state close to the main barrier. Finally, in the non-hydrated systems, all Φ/Ψ fluctuations become slightly increased.

The graphical representation of the complex in orientation (I) in its free energy minimum (Fig. 9), shows the inositol group looking-out of the OH-side of αCD while the phosphate group is found inside the cavity. Hydrocarbon chains are bent towards the mOH side of αCD. The inositol ring is oriented with its normal vector almost perpendicular to the main axis of αCD. The stability of this PI-αCD complex was assessed by a 350 ps trajectory at 300 K which showed no dissociation. (In contrast, the partially complexed state is unstable and evolves towards loose association.) The average structure of αCD calculated from this dynamics highlights a change in the shape of the cavity. Upon inclusion of PI, its geometry has changed from circular to elliptical with $O_{(4)}$ distances of 7.84 Å measured between residues 3,6 and ~8.5 Å beween residues 1,4 and 2,5. In the case of orientation (II), no dissociation was observed when the hydrated system was initially forced into either the partially or fully complexed state.

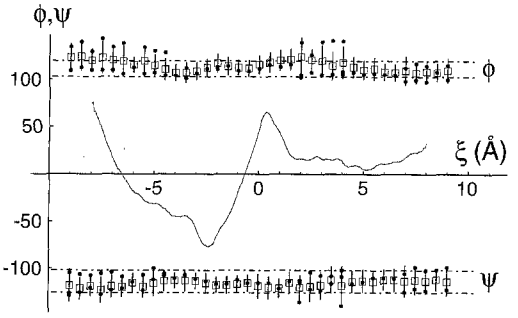

Fig. 8 Behaviour of Φ/Ψ dihedral angles in αCD (see Fig. 1) observed, in the presence of solvent, during 15 ps dynamics trajectories along the ξ reaction coordinate for orientation (I): (αCD)-mOH↔inositol-(PI). *Squares* and *error bars* represent the mean value and r.m.s. deviation of each dihedral angle. *Dots* indicate the position of the deteced "significant peaks" in the Φ/Ψ distribution and *dashed lines* represent the reference Φ/Ψ values found in minimized αCD in vacuum. The shape of the corresponding free energy profile is recalled

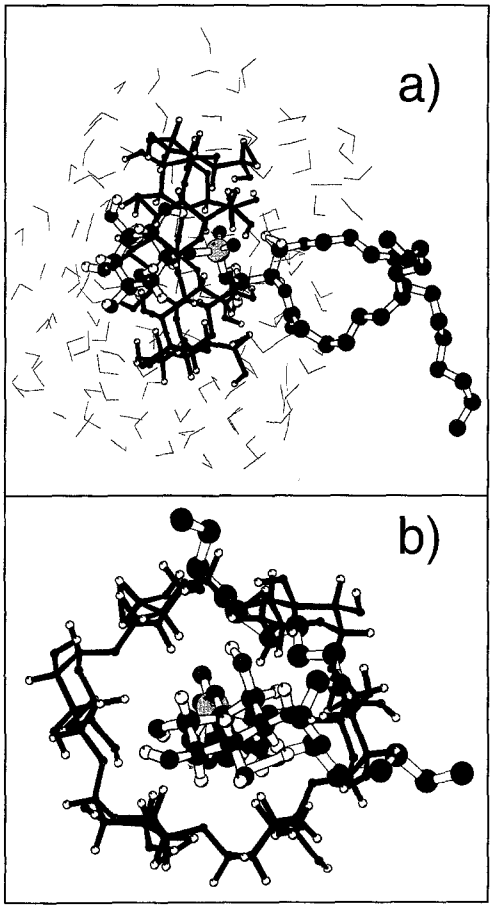

Fig. 9 a, b Ball and stick representation of αCD and PI in the proposed fully complexed state. (orientation (I): (αCD)-mOH↔inositol-(PI), reaction coordinate $\xi \simeq 2.5$ Å). Bonds are drawn in *black* for αCD and in *white* for PI. Figures are generated using MOLSCRIPT (Kraulis 1991) and centered around the P atom of PI coloured in light gray. **a** View in the z-x plane. H_2O molecules of the hydration sphere are drawn as thin wires. **b** View in the plane normal to the z axis. Note the elliptical shape of αCD

Discussion and Conclusion

In the literature, three possible mechanisms of interaction between αCD and lipids are described: i) loose external association. ii) inclusion of lipid chains into the αCD cavity. iii) Formation of an inclusion complex between the phospholipid headgroup and αCD. One of the goals of the present theoretical study was to check these mechanisms and to discuss their possible extension to a macroscopic αCD-membrane interaction.

Electrostatic potential maps demonstrating the polar character of both molecules and their electric dipole moment vectors which are found to be almost parallel to their main axis both suggest the following interaction scheme: assuming that PI is located inside a membrane bilayer, only the lipid headgroup is accessible to an αCD molecule present in solution. The negative charge "seen" by αCD favours a mutual attraction with the primary hydroxyl side of αCD oriented towards the PI headgroup (referred to as orientation I) and parallel alignment of the dipole vectors. For the reverse orientation (orientation II), one expects a global repulsive force betwen the two molecules. This behaviour was indeed observed on "first approach" MD trajectories with the two molecules initially separated by a distance ξ=40 Å. Lipid tails, in those simulations, were fixed to prevent the molecule from rotating and moving around rapidly as is the case inside a membrane but steric hindrance of the other lipids around it was not accounted for.

The complexation of PI and αCD as well as the extraction of the lipid from the membrane have been experimentally observed by ^{1}H and ^{31}P-NMR performed on αCD added to unilamellar vesicles of PI in aqueous solution (Fauvelle et al. 1994). Close spatial distances between H atoms of the inositol group of PI or *myo*-inositol phosphate (Crouzy et al. 1996) and $H_{(3)}$ and $H_{(5)}$ in αCD could account for the corresponding resonance shifts, classically indicating the formation of an inclusion complex, in the NMR study of Fauvelle et al. (1994). This experimental study also reveals implication of $H_{(1,\,2,\,4)}$ atoms of αCD (located on its outer surface) that can be explained either by a transitory conformation of PI located at $\xi \sim 3-4$ Å (in front of the mOH side) prior to the inclusion step or by an external association (Wood et al. 1977). On the PI side, experimentally observed resonances corresponding to either the inositol group or the lipid tails support our hypothesis of a headgroup inclusion and are also compatible with the observation of temporary inclusion of one lipid chain during *distant approach* dynamics trajectories of free PI. These simulations also revealed another possible interaction between αCD and PI: a loose external association of the two molecules stabilized by the antiparallel arrangement of the dipole moments and hydrogen bonding between the secondary hydroxyl group of one glucose residue and the glycerol-phosphate part of PI. However it seems unlikely that this type of association can account for the strong headgroup dependence of αCD-lipid complexation reported by other authors (Fauvelle et al. 1994;

Szejtli et al. 1986). Moreover, for a lipid which is initially located in the membrane, only the headgroup can be accessed by αCD and external association could only take place on a later stage, once the lipid has been isolated from the membrane.

Experimentally, complexation inside αCD, is observed with either charged or neutral substrates (Bergeron et al. 1978). Numerous examples of complexation of αCD with aromatic guest molecules can be found (Wood et al. 1977; Tabushi et al. 1978; Cramer et al. 1967). The *myo*-inositol ring in a chair conformation with H and OH groups lying on different planes, occupies nearly the same lateral space as the overall flat structure of aromatic rings carrying additional alkyl groups. The latter being still included into αCD, the inclusion of inositol into αCD seems thus sterically possible. It is surprising to note that for inclusion, in some cases the "narrow" (mOH) side of αCD is favoured (Uekama et al. 1978; Gelb et al. 1979).

In the study of the short range interaction mechanism, the reaction coordinate ξ was designed to monitor a possible inclusion reaction of PI into the αCD ring. Two orientations of αCD with respect to PI are defined with the inositol group of PI interacting with the primary (I) or secondary (II) hydroxyl group of αCD. Minimum energy profiles showed the existence of two main energy barriers for each of the two orientations. The first, corresponding to the penetration of the inositol group into the cavity, has a height of ~40 kcal/mol which suggests the absence of important steric hindrance during the complexation. The second energy barrier appears when the hydrocarbon chains are enforced through the cavity. These energies are significantly higher than those at the entrance barrier owing to strong VDW contacts between the methyl and glucose groups demonstrating that PI will rather escape αCD from the side where it entered. An increase of the electrostatic interaction energy, when PI has overcome the entrance barrier, has been observed for orientation (II). On the contrary, a decrease is found for orientation (I). This indicates that, even for short range interactions, orientation (I) remains electrostatically more favourable than orientation (II).

To study the effect of hydration on our model, a hydration sphere of explicit water molecules has been used. Free energy calculations requiring very intensive calculation of trajectories, the number of water molecules had to be kept to a minimum and the reaction pathway cannot yet be analysed considering full PI-αCD interactions with membrane and solvent. A simplified model retaining part of PI-αCD interactions with waters was elaborated. It is thought to be a good compromise, to assure hydration of polar groups at reaction coordinates close to the main barrier position ($\xi \sim 0$ Å) while non-polar lipid tails remain outside the hydration zone. αCD is entirely immersed into the solvent sphere while only the inositol-phosphate part of PI is in contact with water (for $\xi < 3$ Å, the glycerol group and hydrocarbon chains become progressively hydrated).

The umbrella sampling technique has been successfully applied to build free energy profiles. This method was especially useful near the tops of the barriers, regions where the sampling of the reaction coordinate would have been inefficient without a biasing potential. For both orientations, an increase in free energy of the fully complexed state with respect to the partially complexed state is found. One may suggest an increase in internal energy and/or decrease in entropy of the waters due to the fact that, when PI is pushed inside the solvent sphere, some waters reach the solvent boundary and feel a strong boundary potential.

The main free energy barrier (leading to the fully complexed state) computed for orientation (II) is very high and the corresponding transition rates are unrealistically slow. On the other hand, for orientation (I), the height of the entrance barrier corresponds to recombination rates on the sub-second to ms time scale compatible with observations made by other authors (Wood et al. 1977; Fauvelle et al. 1994) and will be consequently discussed further.

The study of the Φ/Ψ-dihedral angle fluctuations in "free" αCD shows that glycosidic bond dihedrals are distributed into two populations, noted 1 and 2. On average, $\Phi_1 = -\Psi_2$ and $\Psi_1 = -\Phi_2$ which shows the geometrical equivalence of Φ and Ψ in the ring. The conformation of these dihedral angles can be regarded as one of the most important parameters in the characterization of conformational changes of αCD induced by inclusion (Wood et al. 1977). During full complexation with PI following the ξ reaction coordinate in the (CD)-mOH $\leftrightarrow$ inositol-(PI) orientation, Φ/Ψ undergo important transitions, namely a clear increase in their fluctuations before overcoming the main energy barrier followed by a "freezing" of these fluctuations in the energy minimum of the complex. It seems possible that the *conformational searching* of αCD during the penetration of PI helps the lowering the free energy barrier by an increase of entropy. This hypothesis is corroborated by small Φ/Ψ r.m.s. fluctuations and a high barrier observed for orientation (II). On the other hand, near the fully complexed state, the intermolecular interactions constraint Φ/Ψ to a single narrow population, without introducing forces that would lead to an important rise of the total free energy in the minimum. The loss of vibrational freedom of αCD after complexation and the resulting important entropic changes were also experimentally observed for either neutral or ionic substrates by other authors (Gelb et al. 1979; Bergeron et al. 1978).

Several limitations to our model should remain in mind: first, the sampling of the conformational space available to the system may be insufficient; then, the size of the hydration sphere around αCD is small compared to the cut-off distance, which might introduce artifacts in the calculations. However, we have made test calculations in vacuum which gave free energy barriers very similar to those presented above and therefore, we think that the qualitative information that we draw from this *minimum hydration* system is correct. Our model cannot account directly for the hydrophobic effect on the lipid tails, since they are not hydrated. However, it is known that water forms "ice-like" clusters near nonpolar groups and that breaking of these structures, namely by formation of an inclusion complex, results in a decrease in enthalpy (Némethy and Scheraga 1962). This process is a major driving force for complex formation with αCD (Tabushi et al. 1978). Even if

one considers no explicit inclusion of the lipid tails, the formation of a complex where the lipid headgroup is included inside αCD brings the nonpolar hydrocarbon chains close to the polar parts of αCD. In this case, strong interactions of the polar groups of αCD with water will disturb the structure of water-clusters around the nonpolar parts of the PI molecule (Némethy and Scheraga 1962). Moreover the gain in entropy and hydrogen bonding of "activated" water molecules being expulsed from the αCD cavity upon inclusion complex formation (Tabushi et al. 1978; Saenger 1980) as well as the release of strains present in the hydrated αCD structure (Manor and Saenger 1974; Koehler et al. 1988) are also favourable to the formation of a complex.

Acknowledgements M. Göschl was partially supported by the Deutsch-Französisches Hochschulkolleg foundation.

References

Bergeron RJ, Channing MA, McGovern KA (1978) Dependence of cycloamylose-substrate binding on charge. J Am Chem Soc 100: 2878–2883

Berne BJ, Borkovec M, Straub JE (1988) Classical and modern methods in reaction rate theory. J Phys Chem 92: 3711–3725

Brooks CL, Karplus M (1983) Deformable stochastic boundaries in molecular dynamics. J Chem Phys 79: 6312–6325

Brooks BR, Bruccoleri RE, Olafson BD, States DJ, Swaminathan S, Karplus M (1983) CHARMM: a program for macromolecular energy, minimization, and dynamics calculations. J Comp Chem 4: 187–217

Cramer F, Saenger W, Spatz HC (1967) Inclusion compounds. XIX. The formation of inclusion compounds of α-cyclodextrin in aqueous solutions. Thermodynamics and kinetics. J Am Chem Soc 89: 14–20

Crouzy S, Woolf TB, Roux B (1994) A molecular dynamics study of gating in dioxolane-linked gramicidin A channels. Biophys J 67: 1370–1386

Crouzy S, Fauvelle F, Debouzy JC, Göschl M, Chapron Y (1996) Investigation of the α-cyclodextrin-myo-inositol phosphate inclusion complex by NMR spectroscopy and molecular modeling. Carbohydr Res (in press)

Dewar M, Thiel W (1977) Ground states of molecules 38. The MNDO method. approximations and parameters. J Am Chem Soc 99: 4899–4907

Elder M, Hitchcock P, Mason R, Shipley GG (1977) A refinement analysis of the cristallography of the phospholipid, 1,2-dilauroyl-DL-phosphatidylethanolamine and some remarks on lipid-lipid and lipid-protein interactions. Proc R Soc Lond A 354: 157–170

Fauvelle F, Debouzy JC, Nardin R, Gadelle A (1994) Nuclear magnetic resonance study of a polar headgroup determined α-cyclodextrin-phospholipid association. Bioelectrochem Bioenerg 33: 95–99

Gelb RI, Schwartz LM, Johnson RF, Laufer DA (1979) The complexation chemistry of cyclohexaamylose. 4. Reactions of cyclohexaamylose with formic, acetic, and benzoic acids and their conjugate bases. J Am Chem Soc 101: 1869–1874

Hansbro PM, Byard SJ, Bushby RJ, Turnbull PJH, Boden N, Saunders MR, Novelli R, Reid DG (1992) The conformational behaviour of phosphatidylinositol in model membranes: H-NMR studies. Biochim Biophys Acta 1112: 187–196

Hingerty B, Saenger W (1975) Disorder in a hydrophobic cage illustrated by X-ray structure of α-cyclodextrin-methanol pentahydrate adduct. Nature 255: 396–397

Irie T, Otagiri M, Sunada M, Uekama K, Ohtani Y, Yamada Y, Sugiyama Y (1982) Cyclodextrin induced hemolysis and shape changes of human erythrocytes in vitro. J Pharm Dyn 5: 741–744

Jorgensen WL, Chandrasekhar J, Madura JD, Impey RW, Klein ML (1983) Comparison of simple potential functions for simulating liquid water. J Chem Phys 79: 926–935

Koehler JEH, Saenger W, van Gunsteren WF (1987) A molecular dynamics simulation of crystalline α-cyclodextrin hexahydrate. Eur Biophys J 15: 197–210

Koehler JEH, Saenger W, van Gunsteren WF (1988) Conformational differences between α-cyclodextrin in aqueous solution and in crystalline form. A molecular dynamics study. J Mol Biol 203: 241–250

Kramers HA (1940) Brownian motion in a field of force and the diffusion model of chemical reactions. Physica 7: 284–304

Kraulis PJ (1991) A program to produce both detailed and schematic plots of protein structures. J Appl Cryst 24: 946–950

Manor PC, Saenger W (1974) Topography of cyclodextrin Inclusion complexes. III. Crystal and molecular structure of cyclohexaamylose hexahydrate and the $(H_2O)_2$ inclusion complex. J Am Chem Soc 96: 3630–3639

Myles AMC, Barlow DJ, France G, Lawrence MJ (1994) Analysis and modelling of the structures of β-cyclodextrin complexes. Biochim Biophys Acta 1199: 27–36

Némethy G, Scheraga HA (1962) Structure of water and hydrophobic bonding in proteins. II. model for the thermodynamic properties of aqueous solutions of hydrocarbons. J Chem Phys 36: 3401–3417

Ohtani Y, Irie T, Uekama K, Fukunaga K, Pitha J (1989) Differential effects of β- and γ-cyclodextrins in human erythrocytes. Eur J Biochem 186: 17–22

Patey GN, Valleau JP (1975) A Monte Carlo method for obtaining the interionic potential of mean force in ionic solution. J Chem Phys 63: 2334–2339

Rabinowitz IN, Kraut J (1964) The crystal structure of myo-inositol. Acta Cryst 17: 159–168

Saenger W, Noltemeyer M, Manor PC, Hingerty B, Klar B (1976) "induced-fit"-type complex formation of the model enzyme α-cyclodextrin. Bioorg Chem 5: 187–195

Saenger W (1980) Cyclodextrin inclusion compounds in research and industry. Angew Chem Int Ed Engl 19: 344–362

Szejtli J, Cserhati T, Szogyi M (1986) Interactions between cyclodextrin and cell-membrane phospholipids. Carbohydr Polym 6: 35–49

Tabushi I, Kiyosuke Y, Sugimoto T, Yamamura K (1978) Approach to the aspects of driving force of inclusion by α-cyclodextrin. J Am Chem Soc 100: 916–919

Takusagawa F, Jacobson RA (1978) The crystal and molecular structure of α-maltose. Acta Cryst B 34: 213–218

Uekama K, Hirayama F, Matsuo N, Koinuma H (1978) Structural elucidation of the inclusion complex of tolbutamine with α- and β-cyclodextrins in aqueous solution. Chem Lett, pp 703–706

van Gunsteren WF, Berendsen HJC (1977) Algorithms for macromolecular dynamics and constraint dynamics. Mol Phys 34: 1311–1327

Wood DJ, Hruska FE, Saenger W (1977) ^{1}H NMR study of the inclusion of aromatic molecules in α-cyclodextrin. J Am Chem Soc 99: 1735–1740

Woolf TB, Roux B (1994) The conformational flexibility of o-phosphorylcholine and o-phosphorylethanolamine: A molecular dynamics study of solvation effects. J Am Chem Soc 116: 5916–5926